

Behaviour of $[\text{Ru}(\text{CO})_2(\text{MeCO}_2)_2(\text{PBu}^n_3)_2]$ in the Presence of Carbon Monoxide and/or Hydrogen: Crystal Structure of $[\text{Ru}_6(\mu\text{-H})_6(\text{CO})_{10}(\mu\text{-PHBu}^n)(\mu\text{-PBu}^n_2)_2(\text{PBu}^n_3)_2(\mu_6\text{-P})]^*$

Piero Frediani, Mario Bianchi, Antonella Salvini, and Franco Piacenti

Cattedra di Chimica Industriale, Dipartimento di Chimica Organica della Università di Firenze, Via Gino Capponi 9, I-50121 Firenze, Italy

Sandra Ianelli and Mario Nardelli

Istituto di Chimica Generale ed Inorganica della Università di Parma, Centro di Studio per la Strutturistica Diffattometrica del CNR, Viale delle Scienze, I-43100 Parma, Italy

The behaviour of $[\text{Ru}(\text{CO})_2(\text{MeCO}_2)_2(\text{PBu}^n_3)_2]$ in the presence of N_2 , CO , H_2 , or a mixture of the last two gases has been investigated. When heated, especially in the presence of CO and/or H_2 , acetato and phosphido ligands are lost. At higher temperature, under hydrogen, but in the absence of alternative free ligands, a metal cluster hydride derivative, $[\text{Ru}_6(\mu\text{-H})_6(\text{CO})_{10}(\mu\text{-PHBu}^n)(\mu\text{-PBu}^n_2)_2(\text{PBu}^n_3)_2(\mu_6\text{-P})]$, is formed. An X-ray crystal structure analysis has shown that the shape of this metal cluster is 'butterfly' like with two pairs of triangular wings, encapsulating a bare phosphido phosphorus and carrying three bridging phosphides and two terminal phosphine ligands. The sides of the wings not bridged by the phosphido phosphorus are bridged by hydride hydrogens in such a way that the moiety formed by the metal, phosphorus, and hydride hydrogen atoms shows a local non-crystallographic C_2 symmetry. Two carbonyl ligands complete the metal co-ordination about each ruthenium atom except those of the base hinge that are bound to only one carbonyl each.

The hydrogenation of acetic acid to ethyl acetate in the homogeneous phase has been achieved by using $[\text{Ru}_4\text{H}_4(\text{CO})_8(\text{PBu}^n_3)_4]$ (1) as a catalytic precursor.¹ At the end of the reaction the original ruthenium complex is no longer present while $[\text{Ru}(\text{CO})_2(\text{MeCO}_2)_2(\text{PBu}^n_3)_2]$ (2), $[\text{Ru}_2(\text{CO})_4(\text{MeCO}_2)_2(\text{PBu}^n_3)_2]$ (3), and $[\text{Ru}_4(\text{CO})_8(\text{MeCO}_2)_4(\text{PBu}^n_3)_2]$ may be recovered. These last products may be used as efficient catalytic precursors in the hydrogenation under pressure of the carboxylic group, either free or as an ester.^{2,3}

In order to understand the possible role of the above complexes in the hydrogenation of acetic acid, we have investigated their behaviour at different temperatures when kept under pressure of nitrogen, hydrogen, carbon monoxide, or a mixture of the last two. In this way, we hoped to determine the gas composition, pressure, and temperature appropriate for the formation of hydridic derivatives from these precursors.

We report here the results of this type of investigation on $[\text{Ru}(\text{CO})_2(\text{MeCO}_2)_2(\text{PBu}^n_3)_2]$. The evolution of the system has been followed by i.r. spectroscopy in the 2 200–1 500 cm^{-1} region, using a cell capable of withstanding temperatures up to 200 °C and pressures up to 200 atm, directly connected with the reaction vessel where a n-heptane solution of the complex was allowed to equilibrate with gases. After equilibration and recording of the i.r. spectrum, the solution was cooled and the products recovered and identified. Among them a new phosphido hydrido hexanuclear metal cluster was found whose structure, determined by X-ray crystal analysis, is now reported.

Results

Behaviour of Complex (2) under Nitrogen.—The i.r. spectrum of a n-heptane solution of complex (2) (4.66 mmol dm^{-3}) does not show relevant changes when the temperature is increased from 20 to 110 °C. At 120 °C new bands appear at 2 019, 1 949, 1 915, and 1 719 cm^{-1} due to the presence of both (3) and acetic acid. A hydrogen transfer from a donor must have taken

place. The formation of complex (3) increases when the solution is heated to 160 °C; at 180 °C an absorption band appears at 1 754 cm^{-1} suggesting the presence of methyl acetate. Acetic acid, methyl acetate, tri-n-butylphosphine, and linear heptenes are present in the final solution. These results may be rationalized as in Scheme 1 where the solvent acts as a hydrogen donor.

Behaviour of Complex (2) under hydrogen.—The behaviour in n-heptane solution (4.66 mmol dm^{-3}) under hydrogen (100 atm) was investigated between 20 and 200 °C. At 60 °C after 20 h new bands besides those of complex (2) appear, at 1 720 cm^{-1} , which may be attributed to the presence of acetic acid, and at 1 998 and 1 958 cm^{-1} attributable to the presence of $[\text{RuH}_2(\text{CO})_2(\text{PBu}^n_3)_2]$ (4). Compound (4) was isolated and identified through the usual analyses and by analogy of the above i.r. absorption bands with those reported for $[\text{RuH}_2(\text{CO})_2(\text{PEt}_3)_2]$.⁴

By prolonged heating the predominant bands become those due to (4) and acetic acid. The relative intensity of the bands characteristic of complexes (2) and (4) is affected by the hydrogen pressure: the concentration of (4) increases as the hydrogen pressure is increased. After 20 h at 100 °C it appears to be the only complex present. Even at temperatures in the range 140–160 °C it appears stable. After 30 h at 200 °C, under the same pressure of hydrogen, new bands occur at 2 015w and 1 928(sh) cm^{-1} while the intensity of the bands characteristic of complex (4) decreases. The i.r. spectrum at room temperature and atmospheric pressure of the solution recovered after such a prolonged heating at 200 °C shows, besides the bands due to (4), new bands at 2 040w, 2 015w,

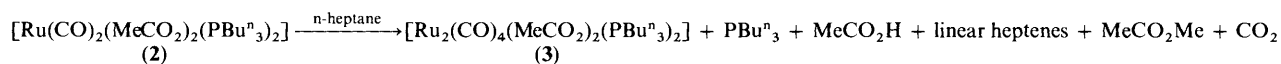
* Supplementary data available: see Instructions for Authors, *J. Chem. Soc., Dalton Trans.*, 1990, Issue 1, pp. xix–xxii.

Non-S.I. unit employed: atm = 101 325 Pa.

Table 1. Atomic co-ordinates ($\times 10^4$) with e.s.d.s in parentheses, for $[\text{Ru}_6(\mu\text{-H})_6(\text{CO})_{10}(\mu\text{-PHBu}^n)(\mu\text{-PBu}^n)_2(\text{PBu}^n)_3(\mu_6\text{-P})]$

Atom	X/a	Y/b	Z/c	Atom	X/a	Y/b	Z/c
Ru(1)	-1 870.1(13)	1 615.3(9)	1 420.2(13)	C(34)	1 497(36)	1 150(19)	6 130(27)
Ru(2)	-231.0(12)	2 154.4(9)	1 325.2(12)	C(35)	601(14)	2 680(10)	3 973(14)
Ru(3)	680.8(12)	1 628.2(9)	2 663.3(12)	C(36)	187(16)	3 049(12)	4 500(16)
Ru(4)	-988.5(12)	2 073.4(9)	2 817.3(12)	C(37)	622(22)	3 582(14)	4 646(19)
Ru(5)	381.2(12)	1 015.8(9)	1 225.0(12)	C(38)	175(22)	3 900(16)	5 212(26)
Ru(6)	-1 487(1)	893(1)	2 743(1)	C(41)	-26(18)	3 356(12)	2 283(18)
P(1)	-576(4)	1 268(3)	2 007(4)	C(42)	-320(22)	3 814(16)	1 580(21)
P(2)	-1 359(4)	2 160(3)	520(4)	C(43)	401(28)	4 197(20)	1 633(28)
P(3)	132(4)	2 073(3)	3 624(4)	C(44)	220(25)	4 607(19)	914(26)
P(4)	-658(4)	2 792(3)	2 101(4)	C(51)	2 233(14)	564(9)	811(15)
P(5)	1 500(4)	1 088(3)	591(4)	C(52)	2 592(20)	545(14)	1 659(20)
P(6)	-2 615(5)	774(3)	3 339(5)	C(53)	3 258(25)	75(17)	1 838(24)
O(1)	-2 006(12)	2 699(10)	3 745(12)	C(54A) ^a	3 748(46)	55(30)	1 250(43)
O(2)	-3 472(11)	2 112(10)	1 169(14)	C(54B) ^a	4 028(48)	281(36)	1 671(51)
O(2A)	-2 267(12)	694(8)	328(11)	C(55)	1 364(15)	1 051(11)	-442(14)
O(3)	685(10)	2 878(8)	465(12)	C(56)	884(19)	1 512(14)	-781(20)
O(4)	2 325(12)	2 088(9)	3 000(12)	C(57)	889(29)	1 544(22)	-1 794(31)
O(4A)	1 075(14)	646(9)	3 614(12)	C(58A) ^b	538(60)	1 301(37)	-1 635(55)
O(5)	-611(12)	457(9)	-68(12)	C(58B) ^b	177(51)	1 274(36)	-2 150(54)
O(5A)	698(15)	-81(8)	1 934(12)	C(58C) ^b	203(41)	1 847(30)	-2 127(39)
O(6)	-449(13)	300(9)	3 991(12)	C(59A)	1 993(14)	1 723(10)	807(15)
O(6A)	-1 580(16)	-104(8)	1 810(15)	C(59B)	2 767(21)	1 780(15)	495(19)
C(1)	-1 621(16)	2 473(12)	3 395(15)	C(59C)	3 141(27)	2 381(21)	739(27)
C(2)	-2 891(16)	1 918(12)	1 278(17)	C(59D) ^a	3 432(55)	2 504(37)	1 423(55)
C(2A)	-2 118(21)	1 046(14)	718(16)	C(59E) ^a	3 638(65)	2 236(46)	1 207(73)
C(3)	283(15)	2 585(11)	751(19)	C(61)	-2 465(19)	544(14)	4 335(20)
C(4)	1 729(14)	1 924(10)	2 886(14)	C(62A) ^a	-2 036(37)	828(29)	4 867(40)
C(4A)	902(16)	1 035(13)	3 268(16)	C(62B) ^a	-2 060(41)	1 155(31)	4 857(43)
C(5)	-245(15)	677(10)	376(18)	C(63A) ^a	-2 202(61)	969(48)	5 669(65)
C(5A)	614(19)	343(12)	1 666(18)	C(63B) ^a	-1 632(47)	660(31)	5 655(48)
C(6)	-831(16)	534(12)	3 526(19)	C(64A) ^a	-1 387(45)	873(32)	6 129(45)
C(6A)	-1 575(21)	281(12)	2 182(20)	C(64B) ^a	-2 209(43)	516(30)	5 953(39)
C(21)	-1 313(13)	1 854(9)	-450(13)	C(65)	-3 203(19)	182(14)	2 990(20)
C(22)	-2 106(15)	1 799(12)	-930(16)	C(66)	-3 537(24)	288(17)	2 093(24)
C(23)	-2 044(18)	1 501(14)	-1 646(20)	C(67)	-3 945(26)	-287(21)	1 639(28)
C(24)	-2 763(24)	1 423(18)	-2 139(23)	C(68A) ^b	-3 492(58)	-548(42)	1 059(60)
C(25)	-1 900(13)	2 808(10)	273(14)	C(68B) ^b	-3 363(58)	-703(42)	1 556(68)
C(26)	-1 526(14)	3 188(11)	-221(14)	C(68C) ^b	-3 197(57)	-827(40)	1 982(59)
C(27)	-1 928(18)	3 729(12)	-338(23)	C(69A)	-3 245(19)	1 369(14)	3 297(20)
C(28)	-1 552(25)	4 080(18)	-889(25)	C(69B)	-4 001(24)	1 292(17)	3 643(23)
C(31)	79(17)	1 715(11)	4 522(15)	C(69C)	-4 614(32)	1 796(22)	3 538(32)
C(32)	843(18)	1 642(11)	5 029(18)	C(69D)	-4 832(37)	1 718(27)	2 752(42)
C(33)	707(19)	1 242(24)	5 682(20)				

^a Site occupancy 0.50. ^b Site occupancy 0.33.

**Scheme 1.**

1 972vw, 1 928w, and 1 922w cm^{-1} due to a new complex which could be isolated from the solution by t.l.c. after neutralization of the acetic acid.

From the analytical results, n.m.r. spectra, and X-ray diffraction structure determination, discussed below, we assign this new product as $[\text{Ru}_6(\mu\text{-H})_6(\text{CO})_{10}(\mu\text{-PHBu}^n)(\mu\text{-PBu}^n)_2(\text{PBu}^n)_3(\mu_6\text{-P})]$ (5).

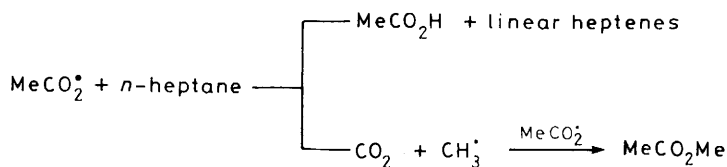
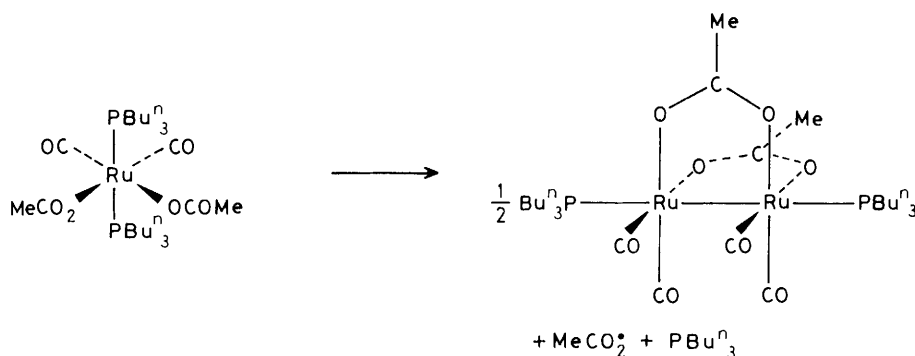
Ethyl acetate was present when the above solutions were heated in the range 160–200 °C.

Behaviour of Complex (2) under Carbon Monoxide.—The i.r. spectrum of a solution of complex (2) (2.93 mmol dm^{-3}) in n-heptane under 60 atm of carbon monoxide remains unaltered below 100 °C. At 100 °C new bands appear at 2 059vs and 1 946vs cm^{-1} which may be ascribed to the presence of $[\text{Ru}(\text{CO})_4(\text{PBu}^n)_3]$ (6)^{5,6} and another band at 1 887s cm^{-1} characteristic of $[\text{Ru}(\text{CO})_3(\text{PBu}^n)_2]$ (7).⁷ After prolonged

heating the bands due to (2) practically disappear while those of (7) are enhanced. On further heating to 140 °C the i.r. spectrum remains unchanged.

Behaviour of Complex (2) under Hydrogen and Carbon Monoxide.—The behaviour of a n-heptane solution of complex (2) (4.65 mmol dm^{-3}) has been investigated under carbon monoxide and hydrogen (80 atm, 1:1 mixture) in the range 20–120 °C. At 60 °C complex (6) is already present together with traces of (7) besides the original (2). Compound (7) becomes predominant after prolonged heating at 100 °C.

X-Ray Crystal Structure Analysis of Complex (5).—Table 1 gives the atomic co-ordinates, Table 2 relevant bond distances and angles. Thermal motion analysis was carried out in the LST rigid-body approximation of Schomaker and Trueblood⁸ considering only the cluster core of the molecule, i.e. the



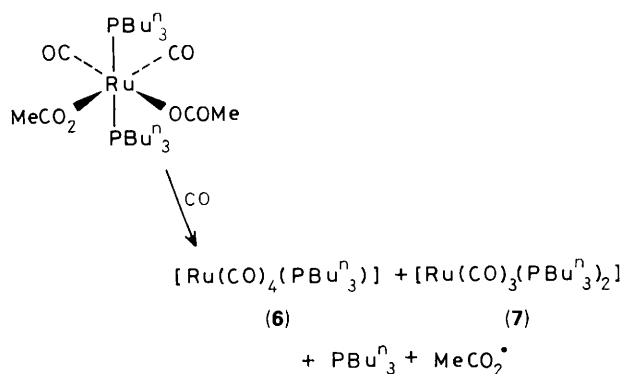
Scheme 2.

ruthenium and phosphorus atoms. The rigid-body fit for this part of the molecule is quite satisfactory, as shown by the value of the $R' = [\sum(w\Delta U)^2/\sum(wU_0)^2]^{\frac{1}{2}} = 0.065$ (U = anisotropic thermal parameter). The corrections of the bond distances are in the range 0.2–2.7 σ and were not considered in the following discussion.

Discussion

Compound (2) if heated in solution, when efficient potential ligands in appropriate concentrations are not available, gives rise to polynuclear complexes. The acetato ligand is lost, involving the reduction of the oxidation state of ruthenium from two to one, and hydrogen is abstracted from the solvent by the acetato radical with formation of an olefin (Scheme 2). The acetato radical may also be decomposed giving rise to methyl acetate (Scheme 2).

In the presence of sufficient carbon monoxide the loss of the acetato and phosphine ligands is compensated by the insertion of CO in the metal co-ordination sphere. Mononuclear complexes of the metal having zero oxidation state are therefore formed and hydrogen abstraction from the solvent takes place (Scheme 3).



Scheme 3.

In our tests the formation of complex (6) from (2) seems to precede that of (7), having a lower content of carbon monoxide, which is the stable form in this condition. This behaviour could be ascribed to an easier reduction of Ru^{II} to Ru⁰ in a monophosphine rather than in a diphosphine intermediate.

In the presence of both carbon monoxide and hydrogen the displacement of these ligands takes place readily at 60 °C, the reaction products being (6) and (7). The presence of hydrogen under pressure together with carbon monoxide evidently eases the elimination of the acetato ligand and the reduction of the central metal atom, as well.

Also in the presence of only hydrogen, when carbon monoxide is not available, the displacement of the acetato ligand takes place at 60 °C with formation of complex (4). Compounds containing both acetato and hydrido ligands have not been identified in the crude product. At higher temperatures, both cluster formation and alkyl-group elimination from the phosphine ligands take place. A phosphine-substituted hydride is formed containing zero-, mono-, di-, and tri-alkyl-substituted phosphine ligands.

Structure of [RuH₂(CO)₂(PBuⁿ)₂] (4).—An octahedral structure containing two phosphine molecules in *trans* position and two hydrogen atoms and two carbonyl groups in *cis* position [Figure 1(a)] may be attributed to [RuH₂(CO)₂(PBuⁿ)₂] on the basis of its i.r., ¹H, ³¹P, and ¹³C n.m.r. data, when compared with those reported for [RuH₂(CO)₂(PPh₃)₂].^{9,10}

The alternative structure [Figure 1(b)] with all equal ligands in *trans* position may be excluded because, due to the presence of a centre of symmetry, it should provide only one active absorption band in the carbon monoxide stretching region, as

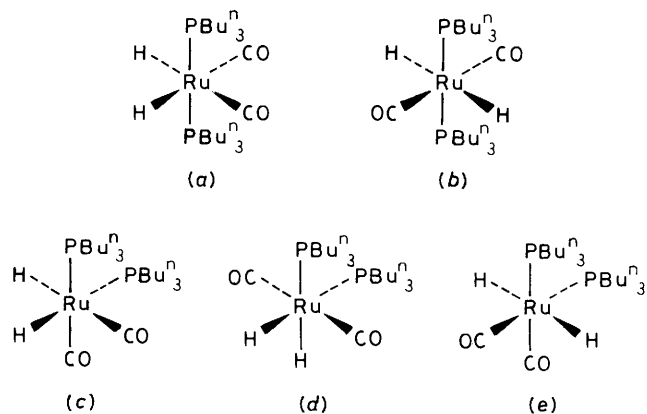


Figure 1. Possible structures of compound (4)

Table 2. Relevant bond distances (Å) and angles (°)

Metal cluster			
Ru(1)–Ru(6)	2.949(3)	Ru(1)–Ru(4)	2.960(3)
Ru(3)–Ru(5)	2.948(3)	Ru(2)–Ru(3)	2.973(3)
av.	2.948(3)	av.	2.966(6)
Ru(2)–Ru(5)	3.020(3)	Ru(1)–Ru(2)	3.155(3)
Ru(4)–Ru(6)	3.040(4)	Ru(3)–Ru(4)	3.132(3)
av.	3.030(10)	av.	3.144(12)
Ru(4)–Ru(1)–Ru(2)	60.6(1)	Ru(4)–Ru(1)–Ru(6)	61.9(1)
Ru(2)–Ru(3)–Ru(4)	60.8(1)	Ru(2)–Ru(3)–Ru(5)	61.3(1)
av.	60.7(1)	av.	61.6(3)
Ru(1)–Ru(2)–Ru(4)	56.6(1)	Ru(1)–Ru(4)–Ru(6)	58.9(1)
Ru(3)–Ru(4)–Ru(2)	57.1(1)	Ru(3)–Ru(2)–Ru(5)	58.9(1)
av.	56.8(2)	av.	58.9(1)
Ru(1)–Ru(4)–Ru(2)	62.8(1)	Ru(1)–Ru(6)–Ru(4)	59.2(1)
Ru(3)–Ru(2)–Ru(4)	62.2(1)	Ru(3)–Ru(5)–Ru(2)	59.8(1)
av.	62.5(3)	av.	59.5(3)
Metal–(μ₆-phosphido)			
Ru(5)–P(1)	2.368(8)	Ru(2)–P(1)	2.604(7)
Ru(6)–P(1)	2.353(8)	Ru(4)–P(1)	2.602(7)
av.	2.360(8)	av.	2.603(7)
Ru(1)–P(1)	2.498(7)		
Ru(3)–P(1)	2.496(7)		
av.	2.497(7)		
Metal–(μ-phosphido)			
Ru(2)–P(2)	2.266(6)	Ru(2)–P(2)–Ru(1)	86.5(2)
Ru(4)–P(3)	2.258(6)	Ru(4)–P(3)–Ru(3)	86.3(2)
Ru(2)–P(4)	2.271(8)	Ru(2)–P(4)–Ru(4)	85.3(3)
av.	2.264(7)	av.	86.2(3)
Ru(1)–P(2)	2.339(8)		
Ru(3)–P(3)	2.322(7)		
Ru(4)–P(4)	2.293(8)		
av.	2.318(13)		
Metal–phosphine			
Ru(5)–P(5)	2.359(8)	Ru(2)–Ru(5)–P(5)	105.7(2)
Ru(6)–P(6)	2.348(9)	Ru(3)–Ru(5)–P(5)	107.7(2)
av.	2.354(8)	Ru–Ru–P av.	108.0(9)
		Ru(1)–Ru(6)–P(6)	108.3(2)
		Ru(4)–Ru(6)–P(6)	110.3(2)
Carbonyls			
Ru–C av.	1.877(17)	Ru–C–O av.	176.0(8)
C–O av.	1.129(11)		
Phosphines			
P–C av.	1.828(11)	Ru–P–C av.	117.3(12)
		C–P–C av.	102.9(14)

against the two of equal intensity observed at 1 998 and 1 958 cm^{-1} . Of the other possible structures containing the phosphine ligands in *cis* position, those having at least one hydrogen atom *trans* to a phosphine [Figure 1(c) and (d)] should be discarded because in the ^1H n.m.r. spectrum of our compound we do not observe absorptions with a coupling constant in the range 70–80 Hz, characteristic for such a hydrogen atom,^{11,12} and also because in the ^{31}P n.m.r. spectrum we observe only one signal, while in the structure of Figure 1(c) the two phosphorus atoms are not equivalent. The structure of Figure 1(e) with two hydrogen atoms in *trans* position must be discarded too because the ^{13}C n.m.r. spectrum of the product shows a triplet at 203.8 p.p.m. ($J_{\text{CP}} = 8.9$ Hz) which may be ascribed to the carbon atoms of the carbonyl groups coupled to the phosphorus atom in *cis* position,¹³ while the structure in Figure 1(e) requires two doublets.

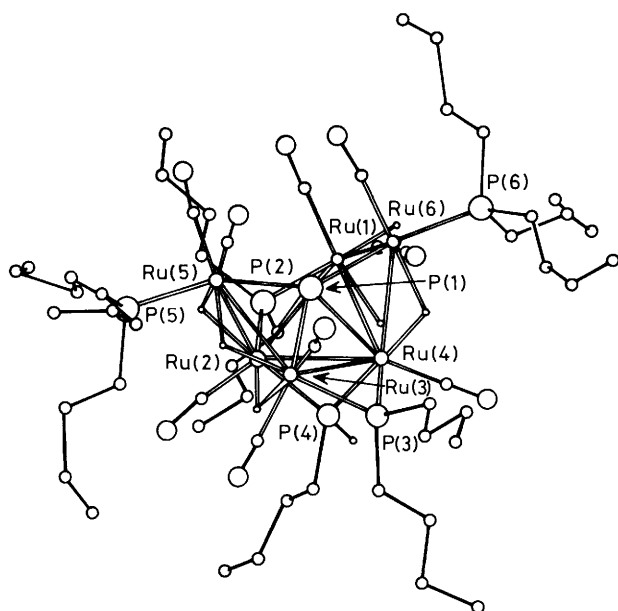


Figure 2. Molecular structure of $[\text{Ru}_6(\mu\text{-H})_6(\text{CO})_{10}(\mu\text{-PHBu}^n)_2(\mu\text{-PBu}^n_3)_2(\mu_6\text{-P})]$. The hydrogen atoms of the *n*-butyl chains are omitted for clarity

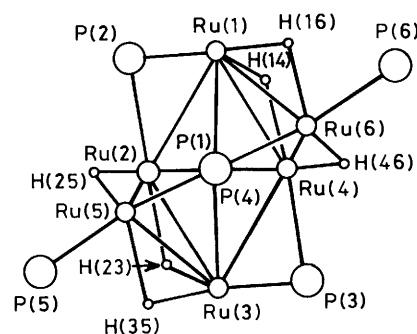


Figure 3. Projection of the cluster along the P(1) ... P(4) direction (only Ru, P, and hydride-H atoms) showing the local C_2 symmetry

Crystal and Molecular Structure of Complex (5).—The crystals are built up of molecules containing 92-electron hexanuclear ruthenium clusters in which three kinds of phosphorus atoms are present: a bare phosphorus partially encapsulated in the metal cluster, three bridging phosphido ligands, and two terminal phosphine ligands. As shown in Figure 2, the shape of the metal cluster is that of a 'butterfly' with two pairs of triangular wings: the first pair hinged on Ru(2)–Ru(4) at a dihedral angle of $124.9(1)^\circ$, the second on Ru(1)–Ru(4) and Ru(2)–Ru(3) at dihedral angles of $122.6(1)$ and $123.6(1)^\circ$, respectively. Alternatively the metal cluster can be described as a tetrahedron [Ru(1), Ru(2), Ru(3), Ru(4)] capped on the [Ru(1), Ru(2), Ru(3)] and [Ru(1), Ru(3), Ru(4)] faces, opened at the [Ru(1), Ru(3)] edge to encapsulate the P(1) atom, or as a trigonal antiprism with [Ru(1), Ru(4), Ru(6)] and [Ru(2), Ru(3), Ru(5)] bases opened at the [Ru(5), Ru(6)] edge to permit entrance of P(1). The metal cluster is essentially built up by triangles which are approximately equilateral (Table 2).

If the *n*-butyl appendices of the phosphine ligands and the carbonyls are not considered, a quite evident local C_2 non-crystallographic symmetry is present with the two-fold axis running along P(1) and P(4), as shown by the projection of Figure 3 and the data of Table 2. From these data it appears that the Ru–Ru distances cannot be considered as all equal, but those involving pairs of ruthenium atoms bridged by the phosphido phosphorus ligands are longer [3.092(3)–3.156(3)

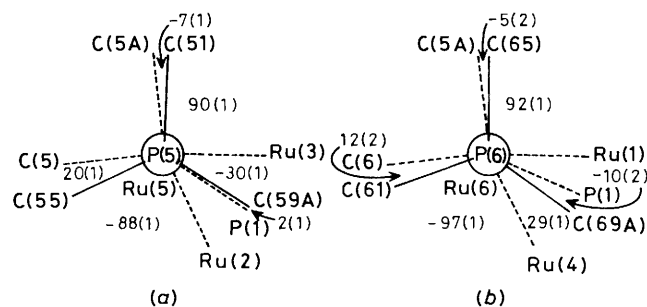


Figure 4. Newman projections along (a) Ru(5)–P(5) and (b) Ru(6)–P(6), showing the orientations of the terminal phosphine ligands

Å] than those bridged by hydrogens [2.948(3)—2.972(3) Å]. These distances are in general longer than those found in $[\text{Ru}_5(\text{CO})_{16}(\mu\text{-PPh}_2)(\mu_5\text{-P})]^{14}$ where the shortest are in the range 2.818(1)—2.831(1) Å and the longest are 2.921(1) and 2.968(1) Å, the latter being between the metal atoms on the edge subtended by the $\mu\text{-PPh}_2$ group.

There are three types of ruthenium atoms differing in their coordination number (c.n.) and environment: (i) Ru(2) and Ru(4) (c.n. = 10) are bound to four ruthenium atoms, one carbonyl, two bridging phosphido phosphorus atoms, the phosphide phosphorus, and two bridging hydrido hydrogens; (ii) Ru(1) and Ru(3) (c.n. = 9) whose first co-ordination sphere involves three ruthenium atoms, two carbonyls, one bridging phosphido phosphorus, the phosphide phosphorus, and two bridging hydrido hydrogens; and (iii) Ru(5) and Ru(6) (c.n. = 8) which have direct interactions with two ruthenium atoms, two carbonyls, one terminal phosphine, and phosphide phosphorus, and two hydrido hydrogens.

As observed for $[\text{Ru}_5(\text{CO})_{16}(\mu\text{-PPh}_2)(\mu_5\text{-P})]$, the phosphide phosphorus does not show equally strong interactions with all metal atoms. Considering the open nature of the cluster, the phosphide atom is only partially encapsulated and its further entry in the cluster is blocked up by the interactions with Ru(5) and Ru(6), as indicated by the fact that the distances of P(1) from the pairs Ru(1), Ru(3) and Ru(2), Ru(4) become proportionally longer in going along the P(1) \cdots P(4) direction: these distances increase linearly with increasing distances of the ruthenium atoms from the plane through P(4) and perpendicular to the P(1) \cdots P(4) direction. Similar to the shortest Ru–P(1) distances are the Ru–P ones when involving the terminal phosphine ligands [2.354(6) Å], while the bridging phosphido ligands form shorter asymmetric Ru–P contacts: 2.264(4) and 2.320(13) Å (average).

The Newman projections of Figure 4 show the orientation of the terminal phosphine ligands with respect to the cluster. The strict correspondence of the two projections is a consequence of the local C_2 symmetry of the cluster.

The disorder found for some butyl chains (common for this kind of ligands) prevented a better refinement of the structure, so no comment is worthy about the bond distances and angles involving carbon atoms.

Experimental

Instruments.—G.l.c. analyses were performed with a Perkin-Elmer Sigma 1 system, gas chromatography–mass spectrometry (g.c.–m.s.) using a Hewlett–Packard model 5790 detector connected with a model 5970 capillary gas chromatograph. Proton, ^{13}C , and ^{31}P n.m.r. spectra were registered using either a Varian CFT80 or VXR300 spectrometer; ^1H and ^{13}C spectra were referenced to tetramethylsilane, ^{31}P spectra in p.p.m. downfield from external H_3PO_4 (85%). Molecular weights were determined using a Wescan model 233 instrument, based on the

isopiestic method. Carbon and hydrogen elemental analyses were performed using a model 240C Perkin-Elmer elemental analyzer. I.r. spectra were recorded with a Perkin-Elmer 580B data system.

Materials.—The complexes $[\text{Ru}_4\text{H}_4(\text{CO})_8(\text{PBU}^n)_4]$ (1),¹⁵ $[\text{Ru}(\text{CO})_2(\text{MeCO}_2)_2(\text{PBU}^n)_2]$ (2),¹⁶ $[\text{Ru}_2(\text{CO})_4(\text{MeCO}_2)_2(\text{PBU}^n)_2]$ (3),¹⁷ $[\{\text{Ru}_2(\text{CO})_4(\text{MeCO}_2)_2\}_n]$,¹⁷ $[\text{Ru}_3(\text{CO})_9(\text{PBU}^n)_3]$,⁷ and $[\text{Ru}(\text{CO})_3(\text{PBU}^n)_2]$ (7)⁷ were prepared as described in the literature.

$[\text{Ru}(\text{CO})_4(\text{PBU}^n)_3]$ (6).—This complex was prepared as described by Piacenti *et al.*¹⁸ for its triphenylphosphine analogue. In a stainless-steel autoclave $[\text{Ru}_3(\text{CO})_9(\text{PBU}^n)_3]$ (0.1 g, 0.312 mmol Ru) were placed together with n-heptane (55 cm³) and then carbon monoxide up to 50 atm at 20 °C. The vessel was heated at 100 °C for 48 h. After cooling at room temperature, the gas was vented and a colourless solution recovered. Its i.r. spectrum showed, in the CO stretching region, absorption bands at 2 059s, 1 983m, and 1 946vs cm⁻¹. Poe and Twigg⁵ and Johnson *et al.*⁶ report for the same product, in decalin solution, absorptions at 2 055s, 1 977m, and 1 939vs cm⁻¹.

Test Procedure.—The equilibration experiments were performed in a stainless-steel vessel (125 cm³) equipped with a pressure gauge and two stopcocks. Air was evacuated from the vessel by a vacuum pump, then the n-heptane solution of the complex under examination was introduced by suction and finally the required gas from a high-pressure cylinder.

Solution concentrations, gas pressures, and reaction temperatures are reported in the presentation of results. The reaction vessel was connected by a stainless-steel capillary coil (total volume 2 cm³) to the i.r. cell capable of withstanding pressures up to 200 atm and temperatures up to 200 °C, equipped with sodium chloride windows. The whole system (reaction vessel, coil, i.r. cell) was kept at the same required temperature. All spectra were recorded after abundant flushing of both coil and i.r. cell with the solution from the vessel. The solvent absorption bands were compensated by using a variable thickness cell.

Preparation of $[\text{RuH}_2(\text{CO})_2(\text{PBU}^n)_2]$.—A n-pentane (30 cm³) solution of complex (2) (0.12 g, 0.176 mmol) was introduced by suction in the autoclave (125 cm³) and then hydrogen up to 100 atm at 20 °C. The vessel was heated at 100 °C for 24 h and then cooled at room temperature. The crude product was transferred directly from the vessel under pressure in a Shlenk tube containing a cool (0 °C), stirred n-pentane suspension of anhydrous sodium carbonate kept under nitrogen. The solid, after separation by centrifugation, was treated in the presence of diethyl ether at 0 °C with a 10% solution of H_2SO_4 to pH 1. The presence of acetic acid in the ether extract was shown by g.l.c.–m.s. analyses. Ethyl acetate was detected by g.l.c.–m.s. analyses of the solution of the crude product.

The remaining solution of the crude product, after solvent distillation under reduced pressure, was eluted on a chromatographic column filled with silica gel using light petroleum (b.p. 40–70 °C) as the eluant. The i.r. spectrum of a n-heptane solution of a central fraction of the eluted material showed in the 2 200–1 800 cm⁻¹ region bands at 1 998vs, 1 958vs, and 1 930 (sh) cm⁻¹. After elimination of the solvent by a nitrogen stream and dissolution of the residue in C_6D_6 ^{31}P , ^1H , and ^{13}C n.m.r. spectra were recorded. A singlet at 32.5 p.p.m. was observed in the ^{31}P n.m.r. spectrum while the ^1H n.m.r. spectrum showed resonances at τ 7.8–8.8 (m, 36 H, $\text{CH}_2\text{CH}_2\text{CH}_2\text{P}$), 9.0 (t, 18 H, CH_3CH_2), and 17.9 (t, 2 H, HRu, $J_{\text{PH}} = 25$ Hz). The ^{13}C n.m.r. spectrum in C_6D_6 showed resonances at δ 14.0 (s, CH_3CH_2),

Table 3. Experimental data for the crystallographic analysis

Formula	$C_{54}H_{106}O_{10}P_6Ru_6$
<i>M</i>	1 707.7
Space group	$P2_1/n$
<i>a</i> /Å	17.291(8)
<i>b</i> /Å	24.720(12)
<i>c</i> /Å	17.667(8)
β /°	97.14(1)
<i>U</i> /Å ³	7 493(6)
<i>Z</i>	4
<i>D_c</i> /Mg m ⁻³	1.514
Reflections for lattice parameters } number } θ range/°	21 14–18
<i>F</i> (000)	3 456
Crystal size/mm	0.41 × 0.56 × 0.61
μ /mm ⁻¹	1.327
Absorption correction (min., max.)	0.1142, 0.1365
Scan speed/° s ⁻¹	0.075
Scan width/°	1.60
θ range/°	3–24
<i>h</i> range	–19 to 19
<i>k</i> range	0 to 28
<i>l</i> range	0 to 20
Standard reflection	2 6 4
No. of measured reflections	12 506
Condition for observed reflections	$I \geq 3\sigma(I)$
No. of reflections used in refinement	3 029
<i>R</i> (int)	0.0384
Max. shift-to-error ratio	0.28
Min. and max. height in final difference map/e Å ⁻³	±0.23
No. of refined parameters	610
$R = \sum \Delta F / \sum F_o $	0.0633
$R' = [\sum w(\Delta F)^2 / \sum w F_o^2]^{1/2}$	0.0610
$S = [\sum w(\Delta F)^2 / (N - P)]^{1/2}$ *	2.21
<i>k</i> , <i>g</i> ($w = k/[\sigma^2(F_o) + gF_o^2]$)	0.26, 0.00

* *P* = Number of parameters, *N* = number of observations.

24.6 (t, CH₂CH₂CH₂P, *J*_{CP} = 6.5), 26.6 (s, CH₂CH₂CH₂P), 32.3 (t, CH₂CH₂CH₂P, *J*_{CP} = 14.3), and 203.8 p.p.m. (t, CO, *J*_{CP} = 8.9 Hz). All data are in accord with the suggested formulation [RuH₂(CO)₂(PBuⁿ)₂].

The recovery of the product and all manipulations involved in the analytical procedures had to be done strictly under nitrogen, with rapidity, working at temperatures never exceeding 0 °C because of the poor stability of the product.

Preparation of [Ru₆(μ-H)₆(CO)₁₀(μ-PHBuⁿ)(μ-PBuⁿ)₂(PBuⁿ)₂(μ₆-P)] (5).—A n-heptane (40 cm³) solution of complex (2) (1.2 g, 1.76 mmol) was introduced by suction into a stainless-steel autoclave (150 cm³) and then hydrogen up to 190 atm at 20 °C. The vessel was heated at 200 °C for 27 h and then cooled at room temperature. The i.r. spectrum at room temperature and pressure of the crude product solution kept under hydrogen showed absorption bands due to complex (4), acetic acid, and (5). After elimination of the solvent by distillation under reduced pressure, preparative t.l.c. separation of the residue was performed using alumina as support and n-hexane as eluant. In this way the separation is accomplished among (4), which partially decomposes on the support, (5) and (2).

Compounds (5) and (2) may be recovered from the stationary phase by elution with methylene chloride. The i.r. spectra of a n-heptane solution of the products recovered showed that (4), (5), and (2) are eluted in this order. A purer sample of (5) may be obtained by further t.l.c. purification on silica by using n-heptane as the eluant. The product recovered was dissolved in diethyl ether and crystallized by addition of methanol up to

incipient clouding and then very slow evaporation of the solvent. An orange-red crystalline solid was recovered (Found: C, 39.00; H, 6.55. Calc. for C₅₄H₁₀₆O₁₀P₆Ru₆. C, 38.00, H, 6.25%). *M* 1 506 (4.88 g l⁻¹ in toluene) (calc. 1 707.7). The i.r. spectrum, in n-heptane, in the 2 200–1 500 cm⁻¹ region, showed bands at 2 040vs, 2 015vs, 2 010 (sh), 1 995vw, 1 972s, 1 960s, 1 950s, 1 928s, 1 922s, and 1 885vw cm⁻¹. The ¹H n.m.r. spectrum, in CD₂Cl₂ solution, showed resonances τ 6.5 (d, 1 H, PH, *J*_{PH} = 330 Hz), 7.3–8.9 (m, 66 H, CH₂CH₂CH₂P), 9.1 (t, 33 H, CH₃CH₂), 26.2 (m, 2 H, HRu), 29.0 (m, 2 H, HRu), and 29.8 (m, 2 H, HRu). The number of hydridic hydrogens present was evaluated by ¹H n.m.r. spectroscopy using an equimolecular solution of complexes (5) and (1). The integrals of the hydridic absorptions give a ratio (5)/(1) = 3/2. The ³¹P n.m.r. spectrum, in CD₂Cl₂ solution, showed a second-order spin system A₂MXB₂ with resonances at δ 13.7 (dd, 2 P, PBu₃, *J*_{AM} = 145), 88.7 (tdt, 1 P, P, *J*_{AM} = 145, *J*_{MX} = 13, *J*_{MB} = 6), 155.2 (dd, 1 P, HPBu, *J*_{MX} = 13, *J*_{XB} = 13), and 202.2 p.p.m. (dd, 2 P, PBu₂, *J*_{BX} = 13, *J*_{BM} = 6 Hz). This pattern was well simulated using the couplings and frequencies quoted above. The data are in agreement with the formulation [Ru₆(μ-H)₆(CO)₁₀(μ-PHBuⁿ)(μ-PBuⁿ)₂(PBuⁿ)₂(μ₆-P)].

Crystal Structure Analysis of Complex (5).—The relevant data on the crystal structure analyses are summarized in Table 3. The lattice parameters were refined by a least-squares procedure¹⁹ using the Nelson and Riley²⁰ extrapolation function. The intensities were measured on a Philips PW 1100 diffractometer using Mo-K_{α1} radiation ($\lambda = 0.709 300$ Å). Corrections for Lorentz and polarization effects were applied and absorption was taken into account using the azimuthal-scan method.²¹ The structure was solved by the direct methods of SHELX 86²² and refined by blocked full-matrix least squares, using the SHELX 76²³ program. Disorder of the terminal parts of some butyl chains was taken into account in the refinement carried out anisotropically for the non-H atoms and isotropically for the hydrogens (some of them were placed in calculated positions).

In spite of the disorder which prevented a better refinement, it was surprising to find small residual electron-density peaks in regions quite reasonable to bridging hydride hydrogens whose real presence was confirmed by ¹H n.m.r. spectroscopy. Calculations carried out with the HYDEX program²⁴ confirmed the presence of these hydrogens, giving calculated co-ordinates for them. To obtain further evidence for their presence, two least-squares refinements without and with these hydrogens were carried out, obtaining *R*' = 0.0625 and = 0.0610, respectively and applying the Hamilton significance test.²⁵ The ratio of these values was calculated as 1.0246, while the theoretical value, for 3 029 independent *F_o* values, 610 variables, and 24 as dimension of the hypothesis, at the 0.5% confidence level, is $R_{24,2419,0.005} = 1.0095$, indicating that the addition of the hydride-hydrogen contributions results in a significantly lower *R* factor.

The atomic scattering factors and the anomalous-scattering coefficients were from ref. 26. The calculations were carried out on the GOULD-SEL 32/77 computer of the 'Centro di Studio per la Strutturistica Diffattometrica del C.N.R. (Parma)' and on the CRAY XMP1 computer of the 'Centro Interuniversitario di Calcolo dell'Italia Nord Orientale (CINECA, Casalecchio, Bologna). In addition to the quoted programs, PARST,²⁷ THMV,²⁸ ORTEP,²⁹ and PLUTO³⁰ were used.

Throughout the paper the averaged values are weighted according to the reciprocals of the variances and the corresponding estimated standard deviations (e.s.d.s) are the largest of the values of the 'external' and 'internal' standard deviations.³¹

Additional material available from the Cambridge Crystallographic Data Centre comprises H-atom co-ordinates, thermal parameters, and remaining bond lengths and angles.

Acknowledgements

This work was carried out with the financial support of Consiglio Nazionale delle Ricerche and Ministero della Pubblica Istruzione.

References

- 1 M. Bianchi, G. Menchi, F. Francalanci, F. Piacenti, U. Matteoli, P. Frediani, and C. Botteghi, *J. Organomet. Chem.*, 1980, **188**, 109.
- 2 U. Matteoli, M. Bianchi, G. Menchi, P. Frediani, and F. Piacenti, *J. Mol. Catal.*, 1985, **29**, 269.
- 3 U. Matteoli, G. Menchi, M. Bianchi, P. Frediani, and F. Piacenti, *Gazz. Chim. Ital.*, 1985, **115**, 603.
- 4 J. D. Cotton, M. I. Bruce, and F. G. A. Stone, *J. Chem. Soc. A*, 1968, 2162.
- 5 A. Poe and M. V. Twigg, *Inorg. Chem.*, 1974, **13**, 2982.
- 6 B. F. G. Johnson, J. Lewis, and M. V. Twigg, *J. Chem. Soc., Dalton Trans.*, 1975, 1876.
- 7 F. Piacenti, M. Bianchi, E. Benedetti, and G. Sbrana, *J. Inorg. Nucl. Chem.*, 1967, **29**, 1389.
- 8 V. Schomaker and K. N. Trueblood, *Acta Crystallogr., Sect. B*, 1968, 24.
- 9 C-L. Lee, J. Chisholm, B. R. James, D. A. Nelson, and M. A. Lilje, *Inorg. Chim. Acta*, 1986, **121**, L7.
- 10 S. Cenini, F. Porta, and M. Pizzotti, *Inorg. Chim. Acta*, 1976, **20**, 119.
- 11 J. R. Sanders, *J. Chem. Soc. A*, 1971, 2991.
- 12 B. E. Cavit, K. R. Grundy, and W. R. Roper, *J. Chem. Soc., Chem. Commun.*, 1972, 60.
- 13 P. Frediani, U. Matteoli, G. Menchi, M. Bianchi, and F. Piacenti, *Gazz. Chim. Ital.*, 1985, **115**, 365.
- 14 S. A. MacLaughlin, N. J. Taylor, and A. J. Carty, *Inorg. Chem.*, 1983, **22**, 1411.
- 15 F. Piacenti, M. Bianchi, P. Frediani, and E. Benedetti, *Inorg. Chem.*, 1971, **10**, 2759.
- 16 M. Bianchi, P. Frediani, U. Matteoli, G. Menchi, F. Piacenti, and G. Petrucci, *J. Organomet. Chem.*, 1983, **259**, 207.
- 17 G. R. Crooks, B. F. G. Johnson, J. Lewis, I. G. Williams, and G. Gamlen, *J. Chem. Soc. A*, 1969, 2761.
- 18 F. Piacenti, M. Bianchi, E. Benedetti, and G. Braca, *Inorg. Chem.*, 1968, **7**, 1815.
- 19 M. Nardelli and A. Mangia, *Ann. Chim. (Rome)*, 1984, **74**, 163.
- 20 J. B. Nelson and D. P. Riley, *Proc. Phys. Soc., London*, 1945, **57**, 160, 477.
- 21 A. C. T. North, D. C. Phillips, and F. Scott Mathews, *Acta Crystallogr., Sect. A*, 1968, **24**, 351.
- 22 G. M. Sheldrick, SHELX 86, Program for Crystal Structure Solution, University of Göttingen, 1986.
- 23 G. M. Sheldrick, SHELX 76, Program for Crystal Structure Determination, University of Cambridge, 1976.
- 24 A. G. Orpen, *J. Chem. Soc., Dalton Trans.*, 1980, 2509.
- 25 W. C. Hamilton, *Acta Crystallogr.*, 1965, **18**, 502.
- 26 'International Tables for X-Ray Crystallography,' Kynoch Press, Birmingham, 1974, vol. 4, pp. 99 and 149.
- 27 M. Nardelli, *Comput. Chem.*, 1983, **7**, 95.
- 28 K. N. Trueblood, THMV, University of California, Los Angeles, 1984.
- 29 C. K. Johnson, ORTEP, Report ORNL-3794, Oak Ridge National Laboratory Tennessee, 1965.
- 30 W. D. S. Motherwell and W. Clegg, PLUTO, University of Cambridge, 1976.
- 31 H. Topping, 'Errors of Observation and Their Treatment,' Chapman & Hall, London, 1960, pp. 87 and 91.

Received 11th January 1989; Paper 9/001991